

Enhancement of the Superconducting Transition Temperature in Nb/Permalloy Bilayers by Controlling the Domain State of the Ferromagnet

A. Yu. Rusanov, M. Hesselberth, and J. Aarts

Kamerlingh Onnes Laboratory, Universiteit Leiden, P.O. Box 9504, 2300 RA Leiden, The Netherlands

A. I. Buzdin

CPMOH, U. M. R. 5798, Université Bordeaux I, 33405 Talence Cedex, France

(Received 21 July 2003; revised manuscript received 29 March 2004; published 30 July 2004)

In (S/F) hybrids the suppression of superconductivity by the exchange field h_{ex} of the ferromagnet can be partially lifted when different directions of h_{ex} are sampled simultaneously by the Cooper pair. In F/S/F trilayers where the magnetization directions of the F layers can be controlled separately, this leads to the so-called spin switch. Here we show that domain walls in a single F layer yield a similar effect. We study the transport properties of $\text{Ni}_{0.80}\text{Fe}_{0.20}/\text{Nb}$ bilayers structured in strips of different sizes. For large samples a clear enhancement of superconductivity takes place in the resistive transition, in the very narrow field range (order of 0.5 mT) where the magnetization of the Py layer switches and many domains are present. This effect is absent in microstructured samples.

DOI: 10.1103/PhysRevLett.93.057002

PACS numbers: 74.45.+c, 74.78.-w, 85.25.Hv

Proximity effects between a superconductor (S) and a ferromagnet (F) are the focus of much current research, basically because of the possibilities for several distinct and unusual phenomena. One is due to the fact that the exchange field h_{ex} in the ferromagnet gives rise to an oscillatory damped amplitude of the pairing function. In an S/F/S geometry, this oscillation allows coupling of the superconducting banks with a phase change of π rather than 0 [1,2]. This can be witnessed in a nonmonotonic variation of the superconducting transition temperature T_c as a function of the F-layer thickness d_F [3,4]; or, especially with a weak ferromagnet, in the Josephson current of an S/F/S junction [5,6] or a superconducting quantum interference device [7]. Other phenomena are linked to a situation in which the Cooper pair can sample different directions of h_{ex} within its coherent volume. The best known example is an F/S/F geometry with a thin S layer, in which the magnetization of one F layer can be rotated with respect to the other. The suppression of the order parameter in S will then be larger when both magnetizations are parallel (P) and smaller when they are antiparallel (AP). This so-called spin switch has been discussed theoretically [8,9] and a first experimental realization was recently reported by Gu *et al.* [10]. They used a weak ferromagnet (CuNi) and reported a small but measurable increase of T_c^{AP} with respect to T_c^{P} (the transition temperatures of the P and AP configurations, respectively) of about 5 mK. However, the physics of the problem is more general. A weak ferromagnet is not an *a priori* condition for the effect, and it might even be argued (although this has not been emphasized in theoretical treatments) that ferromagnets with large exchange fields are preferable. Also, the trilayer configuration is not the only one which can invoke different directions for h_{ex} : any domain wall in the fer-

romagnet offers different directions intrinsically, both in the wall and on either side. In claiming a coupling effect between two F layers, it might even be necessary to check the absence of in-plane domain wall effects. Moreover, other mechanisms may be at play; inhomogeneous exchange fields are predicted to induce enhanced superconductivity by spin-triplet excitations [11,12].

In this Letter, we investigate S/F bilayers and show that the domain state of a magnet with strong spin polarization [$\text{Ni}_{80}\text{Fe}_{20}$, Permalloy (Py)] gives rise to an even slightly larger increase in T_c of the superconductor, in our case Nb, than mentioned above. We give a qualitative discussion of the possible mechanism for the effect, which is basically due to a lowered average exchange field seen by the Cooper pair and might either be called an in-plane spin switch or domain wall induced T_c enhancement.

Samples of Nb/Py were prepared by sputter deposition in an ultrahigh vacuum system. They were structured in simple bars of either $0.5 \text{ mm} \times 4 \text{ mm}$ (“large” sample) or $1.3 \mu\text{m} \times 20 \mu\text{m}$ (“small” sample). Contacts were not included in the geometry in order to minimize problems with stray fields from contact pads or arms. Instead, Au contacts for measuring in four-point geometry were added by sputter deposition. The choice of Py as a ferromagnet is dictated by the wish for large h_{ex} (the spin polarization is 45% [13]), but equally by the need of well-defined magnetization switching at low fields. Since an easy axis for magnetization is induced by the residual magnetic fields in the sputtering machine, care was taken to align the long axis of the bars with the easy axis of magnetization \hat{e}_e . Magnetic fields were applied in the plane of the sample, along the bars and therefore along \hat{e}_e . Different layer thicknesses were used for both Nb and Py, which yielded similar results. We concentrate on

samples with both the Nb and the Py thickness around 20 nm.

The zero-field resistance of a large sample of 21 nm Nb on 20 nm Py on a Si substrate [denoted $s/\text{Py}(20)/\text{Nb}(21)$] as a function of temperature is shown in Fig. 1. The transition temperature is around 5.7 K, depressed from the pure Nb value by the proximity of the F layer. The width is about 100 mK. After stabilizing the temperature at around 5.65 K, in the transition region, the magnetic field $\mu_0 H_a$ is swept from 65 mT down to -65 mT and back. The behavior of $R(H_a)$ is shown in Fig. 2. From the positive field side at 15 mT, R initially goes down, shows a small increase around 5 mT, but then goes down again, followed by a steep dip in a very small field regime around $H_{\text{dip}} = -4.2$ mT. Reversing the sweep from the negative field side, the behavior is symmetric, with a resistance dip now at $+4.2$ mT. Also shown in Fig. 2 is the magnetization of the sample at 8 K, normalized by the saturation magnetization M_s . The loop width is about 8 mT and the switch is quite sharp, although some rounding can be seen close to the coercive field which is due to the misalignment of the easy axis by a few degrees. It is clear that the deep dips in $R(H_a)$ occur precisely at the switching field of the magnetic layer, which indicates that the domain state of the ferromagnet is involved, which is most prominent in the steep part of the magnetization reversal. Since the dip is very pronounced, we can also measure $R(T, H_{\text{dip}})$ and compare this with $R(T, 0)$ in Fig. 1. We find that $R(T, H_{\text{dip}})$ lies consistently *below* $R(T, 0)$, with a maximum difference of about 10 mK. Several samples were measured which all show the same effect, and one data set for a sample $s/\text{Nb}(19)/\text{Py}(20)$ (reversed Nb and Py) is shown in Fig. 3. Again the deep dips in $R(H_a)$ (inset in Fig. 3) are clearly present, although there are differences in the details. For instance, T_c is somewhat lower, around 4.85 K, presumably because Nb layer is slightly thinner. Also, the transition is sharper, with a width of 50 mK. This necessitates a temperature stability during the field sweep of better than 1 mK. The magnetization loop (not shown) is also

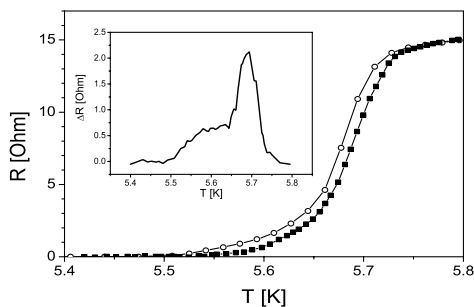


FIG. 1. Resistance R versus temperature T of the large sample $s/\text{Py}(20)/\text{Nb}(21)$ in zero field (open symbols) and in a field of 4.2 mT (filled symbols). The inset shows the difference between the two data sets.

wider, about 14 mT, and the rise in $R(H_a)$ before the dip is reached is higher as well. We make some remarks concerning the details of $R(H_a)$ at the end of the Letter. The main point here is that, again, $R(T, H_{\text{dip}})$ lies consistently *below* $R(T, 0)$, with a smooth behavior of the difference.

The basic explanation we want to offer for our observations is that domain walls are formed in the Py layer during the switching of the magnetization and that these domain walls lead to the enhanced superconductivity. In order to argue this better, we performed measurements on two other types of samples. Figures 4(a) and 4(b) show $R(H_a)$ data (in the transition) on a *small* ($1.5 \mu\text{m} \times 20 \mu\text{m}$) sample $s/\text{Nb}(17)/\text{Py}(20)$ where no effect is found. The other is a large sample $s/\text{Nb}(20)/\text{AlOx}(8)/\text{Py}(20)$, where a thin Al layer was deposited and oxidized before the Py layer was grown. No dips are found, but instead a small resistance increase is seen in the field region of the Py loop, probably due to the effect of stray fields from the magnetic layer on the superconducting layer. This shows that a proximity coupling is necessary for the dips to occur.

Before discussing the effects of domain walls on the superconductivity in more detail, it is necessary to address the characteristics of the walls. For the film thicknesses d_F we use (around 20 nm), they are believed to be of Néel-type: the rotation of the magnetization occurs in the plane of the sample rather than out of plane (Bloch wall), with the transition between the two at thicknesses around 40 nm [14,15]. We note that the magnetic flux coming out of a Bloch wall would suppress the superconductivity rather than do the opposite. The other important parameter is the width δ_w of the walls, which in Py is large due to the small magnetic anisotropy. For Bloch walls, δ_w is of the order of $0.5 \mu\text{m}$, for Néel walls and the case that $d_F \ll \delta_w$ it is of similar magnitude. A detailed study by scanning electron microscopy with

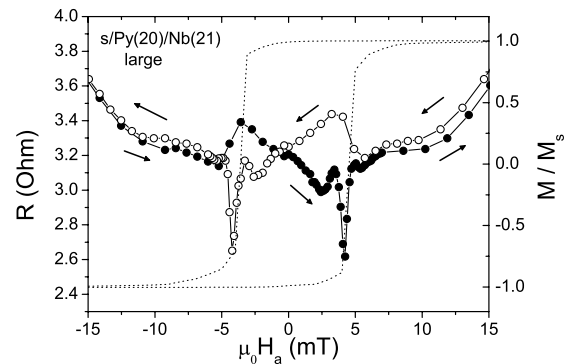


FIG. 2. Left-hand scale: resistance R versus applied field $\mu_0 H_a$ of the large sample $s/\text{Py}(20)/\text{Nb}(21)$. Filled symbols are in the positive field (forward) direction, open symbols in the backward direction. Right-hand scale: magnetization M (dotted lines) normalized on the saturation magnetization M_s versus $\mu_0 H_a$, measured at 8 K. In both cases, $H_a \parallel \hat{e}_e$ (the easy axis of magnetization).

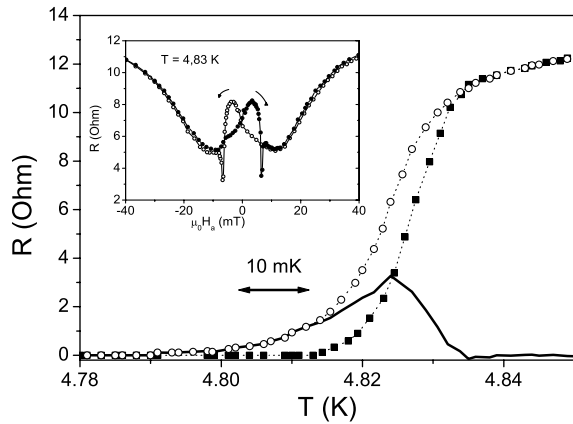


FIG. 3. Resistance R vs temperature T for a large sample $s/\text{Nb}(19)/\text{Py}(20)$ in zero field (open symbols) and in a field of 6.3 mT (filled symbols). The dotted lines are guides to the eye; the drawn line is the difference between the two data sets. Inset: R as a function of applied field $\mu_0 H_a$. The filled symbols are in the forward direction, open symbols in the backward direction.

polarization analysis on thick Py films with surface Néel walls yielded $0.25 \mu\text{m}$ for the half-width of the walls [16]. The fact that δ_w is much larger than the low-temperature coherence length ξ_S of the superconductor (for our Nb, $\xi_S \approx 12 \text{ nm}$) will come back in the discussion. The absence of an effect for the small samples $s/\text{Nb}(17)/\text{Py}(20)$ can be explained by the fact that no stable domains were formed during switching of the magnetization direction. To confirm this assumption, we simulated the switching behavior for a range of Py structures with thickness 20 nm and different size and aspect ratio, using the OOMMF code [17]. Values for the saturation magnetization M_s and the magnetocrystalline anisotropy K_1 were determined from the magnetization measurements and taken to be $M_s = 800 \times 10^3 \text{ [A/m]}$ and $K_1 = 500 \text{ [J/m}^3\text{]}$. The easy axis direction was taken 6.5° away

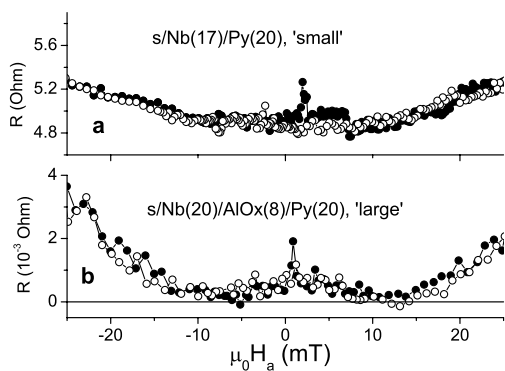


FIG. 4. Resistance R vs magnetic field $\mu_0 H_a$ (a) for a small sample $s/\text{Nb}(17)/\text{Py}(20)$; (b) same for a large sample $s/\text{Nb}(20)/\text{AlOx}(8)/\text{Py}(20)$. The filled symbols are in the forward direction, open symbols in the backward direction.

from the long axis of the structure in order to take the slight sample misalignment into account. Some pertinent results are shown in Fig. 5. In a structure with length ℓ and width w of both $10 \mu\text{m}$, the magnetization loop is small and near the coercive field H_c (around 2 mT) stable domain configurations are present. Upon decreasing w and increasing the aspect ratio $a = \ell/w$, stable configurations no longer occur above $a = 5$. For the $1 \mu\text{m} \times 10 \mu\text{m}$ structure, without a stable domain configuration, H_c has increased to 10 mT. Note that this is still below the value expected for a uniform rotation of the magnetization, which is of order $M_s/2$ according to the Stoner-Wohlfarth model [14], since domains are formed during the switching. The point is that they are not stable. Simulations on structures with larger length (above $50 \mu\text{m}$) showed stable multidomain configurations near H_c even for structures with $a > 10$. It is therefore the combination of small dimensions and large aspect ratio in our small samples which precludes stable domains.

The mechanism we believe to be responsible for the enhancement of the superconductivity in the large samples is basically that the pair breaking experienced by a Cooper pair is smaller when it samples different directions of the exchange field. In a sense, this is the same mechanism as responsible for the F/S/F spin switch, but the simultaneous sampling of two F layers yields a different type of averaging. In order to estimate the effect

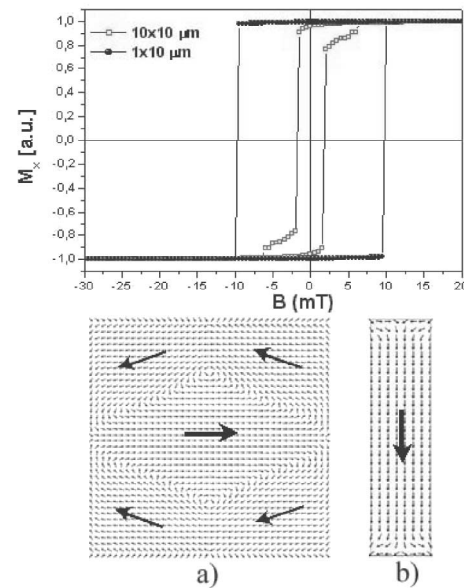


FIG. 5. The switching behavior of small Py structures. The top picture represents magnetization vs external magnetic field for $10 \mu\text{m}$ long Py structures with aspect ratio $a = 1$ (open squares, narrow loop) and $a = 10$ (closed squares, wide loop). The bottom picture shows the correspondent domain configuration near the coercive field for both structures. For samples with the aspect ratio above 2.5 we found no stable multidomain state during magnetization switching.

of the domain wall, we first consider the one-dimensional case of steplike variation of h_{ex} which induces changes in the order parameter over a distance ξ_F (the coherence length in the F layer) leading to a lowered pair breaking parameter in the vicinity of the domain wall [18] and superconductivity which is enhanced with respect to the depression of the uniform F layer. The situation resembles T_c enhancement by twin planes [19,20] and can be treated accordingly. An estimate for the order of magnitude of the enhanced critical temperature T_{cw} can be made as follows. The variation in pair breaking occurring over a distance ξ_F induces a superconducting order parameter over a distance $\xi_S(T_{cw})$ around the wall. In that case, the effective change in pair breaking will be $\xi_F/\xi_S(T_{cw})$, and the T_c enhancement is correspondingly $\alpha \equiv (T_{cw} - T_{cF})/T_{cF} \approx \xi_F/\xi_S(T_{cw})$, with T_{cF} the critical temperature due to the homogeneous suppression of the F layer. Taking into account that $\xi_S(T_{cw}) \approx \xi_S(0)/\sqrt{\alpha}$, we obtain $\alpha \approx [\xi_F/\xi_S(0)]^2$. With $\xi_S(0) \approx 12$ nm and ξ_F for the strongly magnetic Py ≈ 1 nm, the effect is in the range of 1%. The assumption of a steplike change in h_{ex} is not correct, given the large value for δ_w , but it gives a feeling for the orders of magnitude. For larger δ_w , the effect will increase as long as $\delta_w < \xi_S(0)$, but for still larger δ_w it has to decrease to zero again: the Cooper pair cannot sense the variation in h_{ex} any longer. In this limit, the relative increase of T_c is of order $[\xi_S(0)/\delta_w]^2$ [21], which is again about 1%. Another way of arguing that the experiment is sensitive to domain wall formation comes from considering the temperature dependent (Ginzburg-Landau) $\xi_S(T)$ directly. Since we are measuring very close to T_c , ξ_S is actually much larger than the low-temperature value. From a fluctuation analysis of $R(T)$ we estimate T_c to be close to the top of the transition. In Fig. 3 it would be at 4.83 K, where the zero-field and in-field curves start to separate. With a typical transition width of 30 mK, the relative temperature at the zero of resistance $t_r = T/T_c$ is 6×10^{-3} , which makes $\xi_S(t_r) = \xi_S(0)/\sqrt{1-t_r}$ about $0.15 \mu\text{m}$. In the transition, therefore, the condition is $\xi_S(T) \approx \delta_w$, and the Cooper pair samples a considerable part of the rotation of the magnetization. This implies that in the case of Py the in-plane switch will be visible only close to T_c , since at lower temperature the magnetization is homogeneous on the scale of ξ_S . It is of interest to note that enhancement of critical currents below T_c has been reported for the case of Nb/Co, where the domain walls are considerably smaller [22].

Finally, we come back to some details in the $R(H_a)$ data. In Fig. 2, $R(H_a)$ first shows a small peak, before the main dip is reached at a field of opposite sign. We find such a peak present in all measured samples, also when Py is the top layer, although then it is masked by a rise in R

between the main dips. Inspection of $M(H_a)$ shows that deviations from M_s start to occur in this field regime, pointing to initial domain formation and accompanying stray fields probably near the edges of the (necessarily) large samples. While samples with Nb on top show only the small peak, samples with Py on top show a continuous rise in R before the dip field is reached. We believe that either larger roughness or oxidation causes a somewhat different domain configuration and more stray fields in this case. In Fig. 3, R around zero field rises to a value equivalent to R at 20 mT, equal to the rise found in Fig. 4(b) for the sample with an Al oxide layer, indicating a similar amount for the stray fields. A better understanding here must come from samples with a well-defined and engineered domain structure.

This work was supported by the ‘‘Stichting FOM’’ and the European ESF programme ‘‘PiShift.’’ We thank A. Timofeev and S. Habraken for experimental assistance.

-
- [1] Z. Radovic *et al.*, Phys. Rev. B **44**, 759 (1991).
 - [2] E. A. Demler, G. B. Arnold and M. R. Beasley, Phys. Rev. B **55**, 15 174 (1997).
 - [3] L. R. Tagirov *et al.*, J. Magn. Magn. Mater. **240**, 577 (2002).
 - [4] L. Lazar *et al.*, Phys. Rev. B **61**, 3711 (2000).
 - [5] V.V. Ryazanov *et al.*, Phys. Rev. Lett. **86**, 2427 (2001).
 - [6] T. Kontos *et al.*, Phys. Rev. Lett. **89**, 137007 (2002).
 - [7] W. Guichard *et al.*, Phys. Rev. Lett. **90**, 167001 (2003).
 - [8] L. R. Tagirov, Phys. Rev. Lett. **83**, 2058 (1999).
 - [9] A. I. Buzdin, A. V. Vedyayev, and N. V. Ryzhanova, Europhys. Lett. **48**, 686 (1999).
 - [10] J. Y. Gu *et al.*, Phys. Rev. Lett. **89**, 267001 (2002).
 - [11] A. Kadigrobov, R. I. Shekter, and M. Jonson, Europhys. Lett. **54**, 394 (2001).
 - [12] F. S. Bergeret, A. F. Volkov, and K. B. Efetov, Phys. Rev. Lett. **86**, 4096 (2001).
 - [13] J. S. Moodera, J. Nowak, and R. J. M. van de Veerdonk, Phys. Rev. Lett. **80**, 2941 (1998).
 - [14] R. O’Handley, *Modern Magnetic Materials* (Wiley & Sons, New York, 2000).
 - [15] E. Kneller, *Ferromagnetismus* (Springer, Berlin, 1962).
 - [16] M. R. Scheinfein *et al.*, Phys. Rev. B **43**, 3395 (1991).
 - [17] M. Donahue and D. Porter, <http://math.nist.gov/oommf/>.
 - [18] A. I. Buzdin, L. N. Bulaevskii, and S. V. Panyukov, Sov. Phys. JETP **60**, 174 (1984).
 - [19] I. N. Khlyustikov and A. I. Buzdin, Adv. Phys. **36**, 271 (1987).
 - [20] A. A. Abrikosov, *Fundamentals of the Theory of Metals* (North-Holland, Amsterdam, 1988), Chap. 20, p. 489.
 - [21] A. I. Buzdin (unpublished).
 - [22] R. J. Kinsey, G. Burnell, and M. G. Blamire, IEEE Trans. Appl. Supercond. **11**, 904 (2001).